

Temperature Profiles in Hamiltonian Heat Conduction

Jean-Pierre Eckmann^{1,2} and Lai-Sang Young³

¹Département de Physique Théorique, Université de Genève

²Section de Mathématiques, Université de Genève

³Courant Institute for Mathematical Sciences, New York University

We study the Fourier law in the context of Hamiltonian and stochastic models of heat transport with nearest-neighbor coupling, and show that their temperature profiles obey a universal law depending on a single parameter α . This law is linear only when $\alpha = 1$. A large class of Hamiltonian systems allowing for different mechanisms of transport is studied in detail. Different mechanisms are shown to lead to different values of α . We identify a class of translation invariant models with nonlinear temperature profiles, and provide an explanation for this new phenomenon in terms of the Hamiltonian nature of the conductor.

PACS numbers: 05.70.Ln, 05.45.-a

In nonequilibrium physics, the Fourier law is an example of a simple phenomenological principle whose molecular origin is very hard to explain. In essence, it states that for a 1-D object composed of homogeneous material – such as a rod or a thin wire – heat flux is proportional to temperature gradient times heat conductivity. Ever since Fourier's pioneering work [1], many generations of physicists have tried to derive this law from first principles. The current state of the art is summarized in the excellent reviews [2, 3, 4], which all point to the need for a deeper theoretical understanding beyond the many existing models and simulations.

To study the Fourier law in a Hamiltonian context, the most common setting is that of a chain of identical units comprised of disks, plates, penduli, and the like, coupled with short range forces between them. At its two ends, the chain is coupled to mechanisms simulating heat baths maintained at two different temperatures. Because the components of the chain are identical, one may expect heat conductivity to be constant along the chain, so that by Fourier's law, the temperature profile is linear. This appears to be the prevailing thinking behind much of the existing literature. We show in this Letter that the linearity of the temperature profile cannot be taken for granted, even for the very simple systems considered here.

Our two main findings are:

(A) We identify a natural setup that produces nonlinear temperature profiles. For a large class of models that can be regarded as generalizations of [5, 6], we show that *the temperature profile can be linear or nonlinear depending on the nature of the coupling*. The nonlinear profiles are due to a locking mechanism combined with a nontrivial dispersion law. We will explain how, by restricting the motion of tracer particles, the rates of information exchange become velocity-dependent. This, in turn, leads to a *temperature-dependent heat conductivity*.

(B) Our second finding is a *universal law* that holds for very general coupled chains of Hamiltonian systems with *nearest-neighbor* interaction (including those considered in (A)). We show that as the number of constituent cells goes to infinity, the stationary temperature profile is given by

$$T(x) = (T_L^\alpha + (T_R^\alpha - T_L^\alpha)x)^{1/\alpha} \quad (1)$$

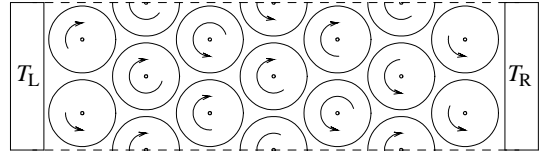


FIG. 1: A typical arrangement of disks in Model H1. The simulations in [6] were done with 2 rows and periodic boundary conditions in the vertical direction, and zig-zag reflecting walls of temperature T_L , resp. T_R , at the two ends. The tracer particle is not shown.

where α is a so-far undetermined constant. Here, T_L and T_R are the temperatures at the left and right ends, and x is the coordinate along the system (normalized to $x \in [0, 1]$). This law does not depend on details of the system aside from translation invariance and energy-scale invariance (meaning in the stationary density, if $E_{i\pm 1}$, the energies at sites $i \pm 1$, are multiplied by λ , then E_i is also multiplied by λ). The value of α in (1), however, depends on the nature of the coupling.

We will elaborate on these findings in the rest of this Letter. Our primary concern here is the temperature profile (TP). The existence of local thermal equilibrium (LTE), which is important for the definition of temperature, will be proved in [7] in the infinite volume limit for some of the models treated here. (For results on LTE for other models, see [8, 9, 10].)

In the models in (A), there is a sharp distinction between *communicating agent(s)* – which we call **tracers** – and *energy storing devices* (ESD). One should think of the tracers as “light” particles interacting with the ESD, which in our case are turning disks with fixed centers. *The value of α will depend on whether the tracers can wander about or are confined to specific regions between the ESD*. It depends also crucially on the *time-of-flight* of the tracers. In a real-world conductor, all these aspects are of course mixed, but for a good theoretical understanding it is useful to separate them. The concepts above are distilled from the following beautiful model:

The MLL Model [5, 6]: We describe this model in some detail, as it contains the basic ingredients of the models in (A). The MLL Model is a purely Hamiltonian model, for which

very careful simulations show that the Fourier law holds, with $\alpha = 1$. The system consists of an arrangement of N disks of radius 1 placed as in Fig. 1, and a little point particle of mass 1 (the tracer) which wanders around the playground, bouncing off the disks [15]. While Fig. 1 suggests a Lorentz gas [11], there is a crucial difference here: Each disk is “nailed down” in its center, around which it turns freely. The state of the system is described by $x = (\omega_1, \dots, \omega_N, q, v)$ where ω_i is the angular velocity of disk i , $q \in \Omega$ is the position of the tracer – Ω is the playground for the tracer, *i.e.*, the physical space occupied by the system minus the disks – and v is its velocity. The phase space of this model is thus $X_{\text{HI}} = (-\infty, \infty)^N \times \Omega \times \mathbf{R}^2$. The disks serve as ESD. When the tracer collides with a disk, the rule of interaction is that of “sticky reflection”: Suppose the angular velocity of the disk being hit is ω , and v_n and v_t are the normal, resp. tangential, component of v relative to the impact point. Then the values of v and ω after the collision are given by the energy and angular momentum conserving law

$$\begin{aligned} v'_n &= -v_n, \quad v'_t = v_t - \frac{2\epsilon}{1+\epsilon}(v_t - \omega), \\ \omega' &= \omega + \frac{2}{1+\epsilon}(v_t - \omega). \end{aligned} \quad (2)$$

Here, $\epsilon \in \mathbf{R}^+$ is proportional to the moment of inertia of the disk divided by the mass of the tracer. [6] treats mostly the case $\epsilon = 1$, where $v'_t = \omega$ and $\omega' = v'_t$, *i.e.*, the two quantities are simply exchanged. Of particular interest to us is the case $\epsilon \ll 1$, which from the tracer’s point of view resembles the classical Lorentz gas.

Remark. The MLL Model, as well as the Hamiltonian models we will describe later, have the following important property: Since there is only a hard-core potential, the time evolution of the system is *rescaled* (by $\sqrt{\lambda}$ when the energy of the particle and the disks are rescaled by λ). In this respect, the model in [6] is very different from models such as the ding-a-ling and ding-dong models [12, 13, 14]. Most importantly, the energies of the tracer and the disks alone determine the time-of-flight of the tracer: It does not depend on the history (as it would in many models considered so far [12, 13, 14]).

We still need to say what happens when the tracer hits one of the ends. In [6], many variants are considered, but for our purpose, the following process is assumed: When the tracer hits one of the ends, it exits the system, and a new tracer is injected into Ω to take its place. The new tracer enters Ω at the point of exit of the old one. Its direction is arbitrary, and its speed is given by the Maxwell distribution for the temperature of the end in question.

Introducing Hamiltonian Models H1 and H2: We now introduce two classes of models both of which have the same basic setup of tracers and turning disks (and the same rules of interaction) as in the MLL Model. These two classes represent, however, two conceptually very different modes of transport. In H1, the communicating agent is, as in MLL, a *single wandering tracer*, while in H2, this role is played by N *locked-in tracers*. We will arrange also for H1 and H2 to have the following properties: (i) they consist of 1-D chains with nearest-

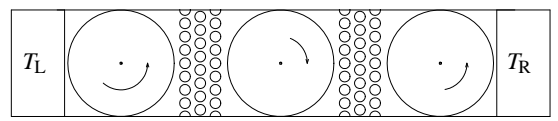


FIG. 2: A sketch of Model H2, when it is made more chaotic. Between the rotating disks, there are disks serving as Lorentz scatterers. The tracers are not shown. The horizontal walls are reflecting.

neighbor interaction, and (ii) as dynamical systems they are very chaotic. Chaotic behavior is used to induce a stronger “memory loss” for the tracer particles and to promote the random mixing of energies. The purpose of (i) and (ii) is to bring these Hamiltonian models closer to their stochastic realizations which we describe below. It is for the stochastic models that (1) will be proven.

Model H1 (wandering tracer): This model will be shown to have a linear TP. Here a single tracer wanders along a chain of boxes separated by walls with a tiny hole that allows the tracer to pass between adjacent boxes. Deep inside each box is a turning disk surrounded by many fixed disks. The turning disk serves as ESD, while the fixed disks are *bona fide* Lorentz scatterers, which serve to randomize the angles of incidence in collisions between the tracer and the turning disk, leading to the exchange of a random portion (*i.e.*, the tangential component) of the energy of the tracer. The smallness of the holes in the separating walls keeps the tracer in each box for a long period. This together with the diffusive action of the Lorentz scatterers ensures that the tracer is equally likely to exit the box from either side [16].

Model H2 (locked-in tracers): This model will be shown to have a nonlinear TP, with $\alpha = \frac{3}{2}$. It consists of a channel exactly one-disk wide, with reflecting boundaries, and with turning disks located at fixed distances apart. These disks turn freely, but they block the channel completely, separating it into individual cells. Inside each cell is a single tracer, which moves back and forth, transferring energy between the turning disks that border the cell [17]. Here one can assume the tracer hits the two turning disks alternately, or, to further randomize the situation, one can add a number of fixed disks in each cell as illustrated in Fig. 2. After hitting one turning disk, the tracer then “gets lost” in this array of Lorentz scatterers, to emerge at some random moment to hit the turning disk at either side with equal probability. In both cases, the time-of-flight of the tracer between hitting turning disks depends only on the speed of the tracer (and not on the state of the disks).

Stochastic realizations of H1 and H2: The stochastic versions of H1 and H2, called S1 and S2, both involve N sites on a 1-D lattice. At site i , $i = 1, \dots, N$, there is a random variable ξ_i representing the energy at site i and taking values in $[0, \infty)$. The heat baths at the ends are modeled by stochastic variables ξ_L and ξ_R which take values in $[0, \infty)$ with a distribution $T_L \exp(-\xi_L/T_L)$, resp. $T_R \exp(-\xi_R/T_R)$ (the Boltzmann constant k_B being set to 1). We identify ξ_L with the variable ξ_0 , and ξ_R with ξ_{N+1} . The rest of the description of Models

S1 and S2 differ.

Stochastic model S1 (corresponding to H1): There are two other random variables, η , to be thought of as the energy of the tracer, and i , which gives the location of the tracer at any given time. The phase space of the system is thus $X_{S1} = \{0, \dots, N+1\} \times [0, \infty) \times [0, \infty)^N$, with $x \in X_{S1}$ given by $x = (i, \eta, \xi_1, \dots, \xi_N)$. We assume that when the tracer is at site i , it interacts with ξ_i . At a site i , $i \notin \{0, N+1\}$, the action is as follows: There is a clock which rings with rate f , for example $f = \eta^{-1/2}$ or $(\eta + \xi_i)^{-1/2}$, representing the time it takes for the tracer to make its way around the i th box. When the clock rings, the following mixing of energies takes place [18]: Choose a random variable p with uniform distribution in $[0, 1]$. Then,

$$\eta' = p(\xi_i + \eta), \quad \xi'_i = (1-p)(\xi_i + \eta). \quad (3)$$

If $i = 0$, η is replaced by a value chosen from the exponential distribution for the temperature T_L . The rule at the right end ($i = N+1$) is similar. After these operations, the tracer jumps with probability $\frac{1}{2}$ to $i-1$ or $i+1$ – except when it is at the ends, in which case it stands still with probability $\frac{1}{2}$ or moves into position 1 (resp. N) from the boundary. *We show in [7] that all such models lead to a linear TP, independently of the waiting function f .*

Stochastic model S2 (corresponding to H2): These models are similar to S1, but now there is one independent variable η_i for *each* pair $(i, i+1)$, $i = 0, \dots, N$, simulating the rattling tracers. Thus, the phase space X_{S2} is $[0, \infty)^{N+1} \times [0, \infty)^N$, where the first $N+1$ coordinates are the ξ_i and the last N are the η_i . Each η_i is equipped with an (independent) clock which rings at an exponential rate proportional to $\eta_i^{-1/2}$. When this clock rings, an exchange of energy involving η_i takes place. For example, η_i exchanges energy alternately with ξ_i and ξ_{i+1} . In another variant, η_i chooses with probability $\frac{1}{2}$ its left or right partner (i.e., ξ_i or ξ_{i+1}), and performs the usual mixing: For example, if ξ_i has been chosen, then

$$\eta'_i = p(\xi_i + \eta_i), \quad \xi'_i = (1-p)(\xi_i + \eta_i). \quad (4)$$

When the clock at site 0 rings, η_0 is replaced by a value chosen from the exponential distribution of temperature T_L as in Model S1. The rule at the right end ($i = N+1$) is similar. Numerical simulations, both for the stochastic and the Hamiltonian model (S2 and H2) show clearly profiles deviating strongly from linearity. They are in perfect agreement with the value of $\alpha = \frac{3}{2}$ predicted by theory (see Fig. 3). Moreover, the local distributions of the ξ_i are canonical.

The qualitative shape of nonlinear profile can be understood easily by considering 3 successive sites, say ξ_{i-1} , ξ_i , and ξ_{i+1} . Since $\xi_{i-1} < \xi_{i+1}$, η_{i+1} rattles faster than η_i (the rate being given by $\eta^{-1/2}$). Thus ξ_i equilibrates more often, and better, with ξ_{i+1} than with ξ_{i-1} . Therefore, ξ_i is closer to ξ_{i+1} than to ξ_{i-1} , which explains the concavity of the TP.

Remarks on model selection: 1) The reductions from H1 and H2 to S1 and S2 are supported strongly by reasoning in agreement with current understanding of dynamical systems,

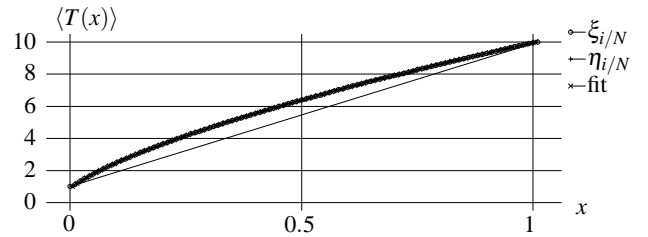


FIG. 3: The mean values of ξ and η , as a function of $x = i/N$, with $T_L = 1$, $T_R = 10$, $N = 100$, averaged over $2 \cdot 10^9$ exchanges of energy according to Model S2. Superposed is the theoretical curve of Eq.(1). Note that the temperature profile is *not* linear and that its curvature is more pronounced at the cold end. Here, $\alpha = \frac{3}{2}$. We have obtained the same profile for many variants of model S2.

although the technology for rigorous proofs is not available at this time. 2) Among the natural models of energy transfer involving tracers and ESD, the ones described above are the simplest – and hence most amenable to analysis – in the sense that the events occurring at the different sites are as *uncorrelated* as can be. 3) An interesting question is what happens in Model S1 in the case of multiple tracers. Here, not only do issues of tracer density enter, but with multiple tracers passing through the same bin with variable time overlaps, the modeling itself becomes more complex.

Sketch of theoretical arguments:

I. Computing the temperature profile in Model S2. Here, we show how Eq.(1) is obtained. Let E_i denote the mean energy (temperature) at site i , and consider 3 successive sites. For illustration we work in Model S2, assuming (i) the tracer visits alternately the left and right disks and (ii) the mixing of energies at each collision is exactly half-and-half. The stationarity condition means that the speed of the tracer is equilibrated as well. Let the mean energy of the left tracer be $\eta_{-, \rightarrow}$ as it heads toward site i and $\eta_{-, \leftarrow}$ as it goes away from it. By the rule of mixing, we have $\eta_{-, \rightarrow} = (\eta_{-, \leftarrow} + E_{i-1})/2$, $\eta_{-, \leftarrow} = (\eta_{-, \rightarrow} + E_i)/2$, leading to $\eta_{-, \rightarrow} = (2E_{i-1} + E_i)/3$, $\eta_{-, \leftarrow} = (E_{i-1} + 2E_i)/3$.

We assume the speed of the tracer is E^γ when E is its energy. The value of γ for Model H2 (and many other models without potential) is $\gamma = \frac{1}{2}$ (since the energy is purely kinetic) while for potential interactions, the time is given by an integral of the form $\int dq (E - V(q))^{-1/2}$, which for large E and $V(q) \sim |q|^m$ behaves like $\mathcal{O}(E^{-1/2+1/m})$, so that $\gamma = \frac{1}{2} - \frac{1}{m}$ [19]. Fixing γ , the average time for a round-trip of the tracer between sites $i-1$ and i is $\tau_- = \eta_{-, \rightarrow}^{-\gamma} + \eta_{-, \leftarrow}^{-\gamma}$, and the rate at which site i gets information from the left is the inverse of this quantity. An entirely analogous reasoning applies on the “+” side. From the stationarity condition, we get

$$E_i = \frac{\tau_-^{-1}(E_i + \eta_{-, \rightarrow})/2 + \tau_+^{-1}(E_i + \eta_{+, \leftarrow})/2}{\tau_-^{-1} + \tau_+^{-1}}. \quad (5)$$

Perform a perturbative analysis at the point $x = i/N$ where N is very large. Then, to second order in $\varepsilon = 1/N$, $E_{i\pm 1} =$

$T(x) \pm \varepsilon T'(x) + \frac{1}{2} \varepsilon^2 T''(x)$, and (5) leads to

$$t = T(x) + \varepsilon^2 \frac{T''(x)T(x) + \gamma(T'(x))^2}{4T(x)} + \mathcal{O}(\varepsilon^4).$$

Since E_i must be equal to $T(x)$, we find

$$T''(x)T(x) = -\gamma(T'(x))^2,$$

the solution of which with boundary conditions $T(0) = T_L$ and $T(1) = T_R$ is Eq.(1) with $\alpha = 1 + \gamma$. Thus, for the cases considered in Model S2, we have $\gamma = \frac{1}{2}$ and $\alpha = \frac{3}{2}$. One also checks that the energy flux is given by $T'(x)\sqrt{T(x)}$ (which is constant along the profile, but *not* proportional to the temperature difference).

Generalization. Note that when $\gamma = 0$, *i.e.*, when the rate at which information is exchanged is independent of energy, then $\alpha = 1$, which indeed gives a linear TP. Note also that our derivation is quite general: if E^γ is replaced by $1/F(E)$, the profile is given by $T''(x)F(T(x)) = (T'(x))^2 F'(T(x))$.

Remark. Many authors have done careful simulations of models that are close to Models H2 or S2, and have observed linear TPs. It should be noted that the profiles predicted by (1) are very close to linear if T_R/T_L is not far from 1. Our theory predicts that deviations from linearity become more prominent with the increase of T_R/T_L .

II. Linear profile in Model S1. The reasoning above is not valid for Model S1, for here it is a single tracer that is responsible for all transmission of information to all sites. The situation is as follows: Given an initial condition $x_0 \in X_{S1}$, the sample paths of the stochastic process are parametrized by (Σ, μ) where $\Sigma = (\{+, -\} \times [0, 1])^\infty$ and μ is the product measure on Σ . Here $\{+, -\}^\infty$ tells us the sequence of “jumps” made by the tracer: \pm means it goes from site i to $i \pm 1$, (at the ends it is only allowed to go in the direction that makes sense, or stand still); and the sequence of $p \in [0, 1]$ are the random variables in the mixing rule in Eq.(3) [20].

Consider first a *fixed-time model*, meaning the tracer makes exactly one jump at each unit of time. In this case the variable i performs a standard random walk on $\{1, 2, \dots, N\}$ (except at the ends), and it is easy to see that it spends an equal amount of time at each of the N sites. Reasoning as above, we see that in the stationary measure, E_i is affected equally by E_{i-1} and E_{i+1} , resulting in a linear profile (that is, $\alpha = 1$).

Model S1 as described earlier is a *skewed-time model*, in the sense that the jumps occur at exponential rates depending on a certain waiting time f . The crucial observation here is that the mixing rule, and hence the outcome of the mixing process, *does not depend on the duration of this waiting time*. Moreover, if the tracer heads left from site i , then it can only return from the left; and similarly for the right. Thus although the tracer may spend a great deal more time at one site than at another, the fact that the probabilities of jumping left and right from site i are equal ensures that the probabilities of returning to site i from the two sides are equal. Hence the TP is linear in this case as well.

Summary and conclusion. (1) We have pinpointed a simple and very natural mechanism responsible for nonlinear temperature profiles in homogeneous conductors, namely that when interacting particles (or springs) are confined to bounded regions of physical space, their interaction speeds become energy-dependent. (2) We have derived an exact formula – a universal law – for the energy profiles of very general chains of Hamiltonian systems with nearest-neighbor interactions. When nonlinear, this law predicts that deviation from linearity increases with the quotient T_R/T_L . (3) Finally, the underlying causes for nonlinearity that we have identified clearly go beyond the models studied here. They suggest that the presence of some (weak) nonlinear effect may be a more common phenomenon than recognized when very disparate temperatures are imposed at the two ends of a 1-D system.

Acknowledgments. We have profited from illuminating discussions with C. Mejía-Monasterio, D. Ruelle, L. Rey-Bellet, O. Lanford, Y. Avron and many others. JPE wishes to thank the Courant Institute and IHES for their kind hospitality. This research was partially supported by the Fonds National Suisse and NSF Grant #0100538.

- [1] J. B. J. Fourier, *Oeuvres de Fourier / pub. par les soins de m. Gaston Darboux, sous les auspices du Ministère de l'Instruction Publique* (Gauthier-Villars et fils, Paris, 1888–1890).
- [2] S. Lepri, R. Livi, and A. Politi, Phys. Rep. **377**, 1 (2003).
- [3] F. Bonetto, J. L. Lebowitz, and L. Rey-Bellet, in *Mathematical physics 2000* (Imp. Coll. Press, London, 2000), pp. 128–150.
- [4] B. Li, G. Casati, J. Wang, and T. Prosen (cond-mat/0307692).
- [5] C. Mejía-Monasterio, H. Larralde, and F. Leyvraz, Phys. Rev. Lett. **86**, 5417 (2001).
- [6] H. Larralde, F. Leyvraz, and C. Mejía-Monasterio, J. Stat. Phys. **113**, 197 (2003).
- [7] J.-P. Eckmann and L.-S. Young, In preparation (2004).
- [8] A. Dhar and D. Dhar, Phys. Rev. Lett. **82**, 480 (1999).
- [9] A. Galves, C. Kipnis, C. Marchioro, and E. Presutti, Comm. Math. Phys. **81**, 127 (1981).
- [10] C. Kipnis, C. Marchioro, and E. Presutti, J. Statist. Phys. **27**, 65 (1982).
- [11] H. Lorentz, Akademie van Wetenschaffen te Amsterdam, Section of Sciences **7**, 438 (1905).
- [12] G. Casati, J. Ford, F. Vivaldi, and W. Visscher, Phys. Rev. Lett. **52**, 1861 (1984).
- [13] T. Prosen and M. Robnik, J. Physics. A **25**, 3449 (1992).
- [14] P. Garrido, P. Hurtado, and B. Nadrowski, Phys. Rev. Lett. **86** (2001).
- [15] More than one tracer is sometimes used in [6], but we will limit ourselves to the single tracer case.
- [16] In [6] several of the considerations above are implemented in a very good compromise between practical feasibility and reasonable mixing between the collisions.
- [17] A version of this model was suggested to us by D. Ruelle.
- [18] Similar stochastic rules for mixing energies are used in [9, 10].
- [19] The case of the hard disks of Model H1 corresponds to $m = \infty$.
- [20] At the ends, we take the exponential distribution.